A Discussion on Fracture Energy of Vertical Joint in Concrete

Ayumi Satoh[1, a], Kanji Yamada[2,b] and Satoru Ishiyama[3,c]

[1]BMR Labs, Akita Prefecture University, Tsuchiya, Yurihonjo, Akita, 015-0055, Japan

[2]BMR Labs, Akita Prefecture University, Tsuchiya, Yurihonjo, Akita, 015-0055, Japan

[3]BMR Labs, Akita Prefecture University, Tsuchiya, Yurihonjo, Akita, 015-0055, Japan

[a]m09c003@akita-pu.ac.jp, [b]kanji_yamada@akita-pu.ac.jp, [c]ishiyama@akita-pu.ac.jp

Keywords: Stress Distribution Model, Tension Softening Diagram, Placing Joint, Strength, Ductility, Fracture Energy

Abstract. This study elaborates tension softening characteristics of placing joint in concrete aiming at revealing some clues for improving mechanical properties of it. The authors conducted fracture mechanics test of six types of concrete prisms which have a vertical placing joint. Tension softening diagrams were obtained from the test, which were used to make a stress distribution model on the joint surface. The authors predicted bending moment in the concerned section and GF with using the proposed model, which showed a good agreement with the experimental ones. The important finding is that GF is proportional to the second power of tensile strength (ft) which derives from the equation drawn by the authors. The results showed that the key to enhance GF is achieving high tensile strength of the placing joint.

Introduction

Every concrete structure has inevitably construction joint that is a discontinuous plane of concrete produced during construction. There are lasting needs for enhancing the adhesion performance of placing joint, but little study is conducted concerning tension softening diagram (TSD). TSD is the most fundamental feature of fracture mechanics parameters [1], and the study of it is inevitable for enhancing structural performances. The authors have studied TSDs of placing joint and pointed out that fracture energy (GF) is strongly related to flexural strength of the specimen with placing joint [2,3]. A stress distribution model is useful for better understanding of TSD because the model should include TSD in it, which is the motivation of this study.

There are many literatures that analyzed the behavior of members with cracks in them with using stress distribution model [4], one of which elaborated size effect of concrete with the model [5]. All of the previous studies use assumptions that the existence of a neutral axis in the section and the linear distribution of strain from the top to the bottom, which the authors used as the assumptions for constructing the model.

This paper aims at expanding the knowledge of TSD with making a stress distribution model which includes TSD in the cracked tensile region.

Experiment and Analysis

Specimens for experiment. The authors prepared five types of specimens with a varied type of placing joint made from different roughening or different form on them, and a type of monolithic specimens for the reference. The specimens' names are N for monolithic ones, J for ones made with joint sheet, E for ones with exposed aggregates on the joint surface, FS for ones with a fractured surface of concrete, R for ones roughened with steel wire brush and SP for ones with an as-cast surface made with a form made of steel plate painted with fluoro-plastic. Table 1 shows mix proportion of concrete used for the specimens, and Table 2 the attribute of specimens.

Table 1 Mix proportion of concrete

W/C	s/a	Weight of materials [kg/m^3]					Air	slump
[%]	[%]	Water	Cement	Sand	Gravel	Ad	[%]	[cm]
51.4	43.0	177	344	739	1010	1.72	3.0	22

Ad: Super Plasticizer

Table 2 Attributes of specimens

Specimen	Surface condition	Elapsed time after 1st cast
N	(Monolithic)	-
J	Joint sheet	24hours
E	Exposed aggregate	24hours
FS	Fractured surface	35days
R	Roughened with steel wire brush	24hours
SP	As cast	24hours

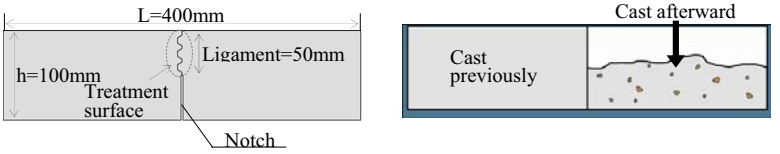

Fig. 1 Detail of specimen (left) and method for producing specimen (right)

The number of specimens was three for each case, which have a section of 100 mm by 100 mm and a length of 400mm. After 24 hours from the 1st cast of concrete in the half part of mold, the joint surface was roughened in the case of R. Then concrete was cast in the remained half of mold as depicted in Fig. 1. The specimens were cured in water at 20°C for 28 days after the final cast of concrete. A 50mm depth notch was incised at the center of the specimen before the fracture mechanics test.

Fracture mechanics test and analysis. Fracture toughness test was executed with observing RILEM's recommendation [6]. Load and crack mouth opening displacement (CMOD) were measured continuously during the loading. To cancel the dead weight of specimen and to obtain a good and precise measurement, a counter weight made of steel was glued at each end of specimens. Servo type loading machine was used to get high-speed response with the help of feed-back system in the machine.

TSD was achieved from the load-CMOD curve of specimen with employing multi-linear approximation method which was standardized by JCI [7]. Fracture energy is consumed energy during the fracture of a section and displayed as an area enclosed with x-axis, y-axis and TSD in the graph, which is abbreviated as GF. Fracture energy consumed until the maximum load is abbreviated as GF_{px} in this study. In Fig. 2, ft is tension softening initial stress which is the same as tensile strength. W_{px} is a crack width when load reaches the maximum value and Wcr is a crack width when load becomes zero (critical crack width).

Experimental Results

Mechanical performance of Joint. Table 3 shows the fracture mechanics parameters. The resulted GFs are ranging from 0.01N/mm (specimen SP) to 0.05 N/mm (specimen J) with a reference result of 0.1N/mm for specimen N. The joints with roughened surfaces such as specimen J, R and E have good results, but the same rough surface did not produce good results for specimen FS. This is due to the elapsed time (35days) for specimen FS that decreases unhydrated cement on the surface of joint.

There are some important remarks to be said regarding Table 3. The ratio of GF from strongest joint divided by that from weakest joint reaches about 10, indicating the adequate roughening is very essential for the enhanced performance of the joint. The interesting finding is that the ratio of Fb or Ft divided by that of weakest joint is about 2 to 3, which is far smaller than that of GF. This result is the same as the one from a previous research by Kurihara [8].

GF at the maximum load. Fig.3 shows TSDs in which the mark • indicates the point when each bending specimen reaches the maximum load, i.e., Wpx. Table 3 indicates that the value Wpx is proportional to the value GF. So it is easy to understand that GF_{px} is proportional to GF, which is shown in Fig. 4. Fig.4 means the total GF is determined when crack width reaches the end of the first branch of TSD, meaning only the first branch is the most important part for fracture toughness. But we do not confuse the fact that this is the case for brittle fracture of joint and not for ductile fracture like fiber reinforced cementitious materials.

Table 3 Fracture mechanics parameters

	fb [Mpa]	ft [Mpa]	Wcr [mm]	W_{Px} [mm]	GF [N/mm]	GF_{Px} [N/mm]
N1	4.94	6.82	0.213	0.011	0.0911	0.0296
N2	4.85	7.07	0.130	0.007	0.0955	0.0261
N3	4.60	7.28	0.224	0.013	0.1160	0.0299
J1	3.74	5.80	0.200	0.007	0.0597	0.0160
J2	3.80	5.56	0.051	0.007	0.0467	0.0169
J3	3.53	4.76	0.117	0.010	0.0501	0.0188
E1	2.85	2.90	0.113	0.007	0.0340	0.0104
E2	3.12	3.92	0.049	0.006	0.0343	0.0119
E3	2.80	3.26	0.083	0.008	0.0372	0.0119
FS1	1.61	2.11	0.094	0.006	0.0243	0.0044
FS2	2.01	2.90	0.088	0.005	0.0211	0.0056
FS3	2.11	2.11	0.105	0.007	0.0288	0.0074
R1	3.42	6.47	0.047	0.003	0.0407	0.0107
R2	3.03	5.68	0.054	0.005	0.0297	0.0101
R3	3.60	5.52	0.038	0.007	0.0336	0.0140
SP1	2.00	3.65	0.028	0.003	0.0112	0.0039
SP2	2.20	3.49	0.027	0.003	0.0129	0.0045
SP3	1.75	3.03	0.071	0.006	0.0131	0.0047

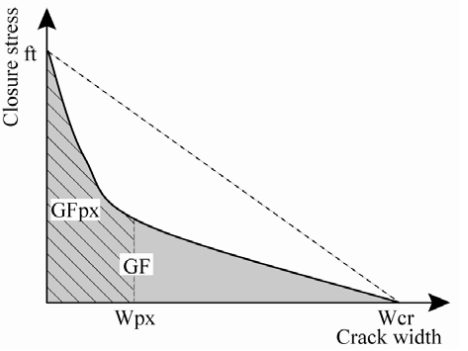

ft: tension softening initial stress
GFpx, Wpx: fracture energy or crack width at maximum load
GF: fracture energy
Wcr: critical crack width

Fig.2 Tension softening diagram

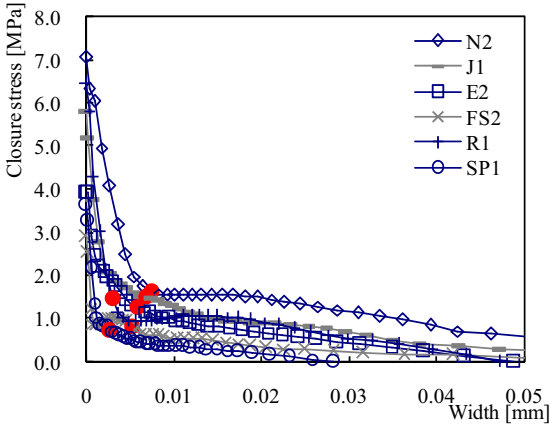

Fig. 3 Tension softening diagrams of specimens

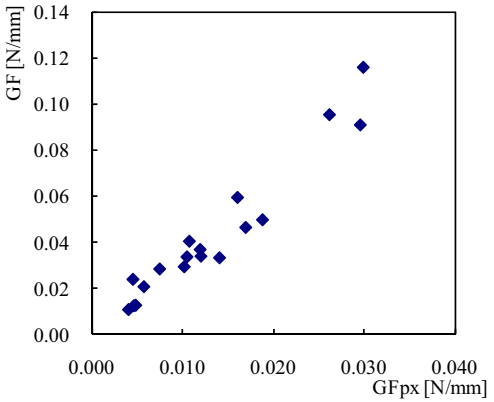

Fig.4 Relationship between GF and GFpx

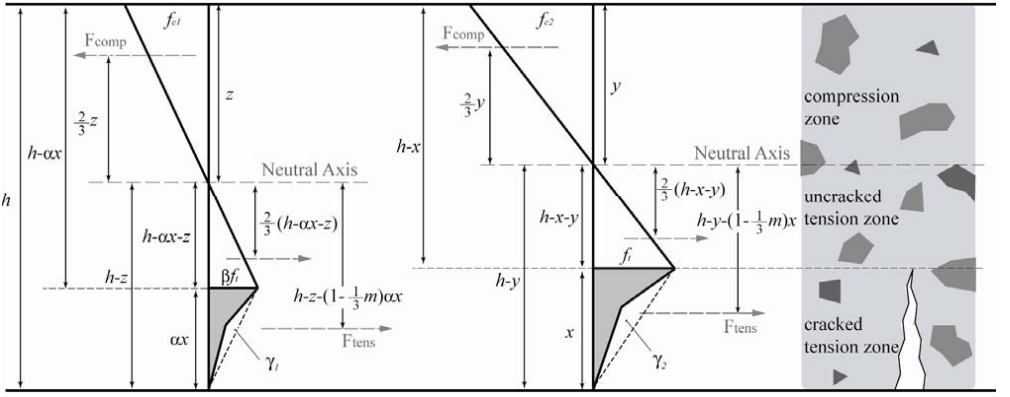

Fig.5 Stress distribution model for specimen 1 (left) and specimen 2 (right)

Composition of Stress Distribution Model

Assumptions for the model. The authors propose a stress distribution model in a ligament of bending specimen at the maximum load which includes TSD in the cracked tensile region, elastic tensile region in the un-cracked region and linear compressive region in Fig. 5. The left hand drawing indicates specimen 1 for the case with a joint, and the right hand drawing the monolithic specimen 2 for the reference (specimen N).

In specimen 1, the cracked region height is α x and the tensile strength that appears at the crack front is β ft, where α and β are ratios of height and strength for specimen 1 to those of specimen 2. The maximum load occurs when the crack height is α x for specimen 1, or x for specimen 2. At this load, the maximum compressive stress f_{c1} (specimen 1) and f_{c2} (specimen 2) occur at the top. The height of neutral axis is z for specimen 1, or y for specimen 2.

Ordinary assumptions for fiber models [9] were adapted to calculate bending moment in the concerned section, as follows;

1) The linear distribution of strain from the top of compressive part to the bottom of tensile part
2) The linear distribution of crack width in the cracked region that produces the real shape of TSD
3) The balance of compressive and tensile total force

The authors simplified the real shape of TSD to the triangular shape for the simple calculation. To avoid large error by this simplification, the values γ and m were introduced. γ is a ratio of real GF divided by the assumed GF of the triangle, and m is a ratio of the arm length of real TSD divided by the assumed one of the triangle. The value m was experimentally set as 1.217 [10].

Calculation of moment for specimen 1. The following equations were drawn for specimen 1 referring Fig.5 and above mentioned assumptions.

The balance of compressive and tensile force in the section leads to the following expression

$$f_{c1} = \frac{\beta f_t}{z}\{h - \alpha x(1-\gamma_1) - z\} \tag{1}$$

The retention of plane in the bending section brings the following expression

$$f_{c1} = \frac{z \cdot \beta f_t}{h - \alpha x - z} \tag{2}$$

As f_{c1} in Eq. 1 and Eq. 2 is the same, then making them equivalent, so that z is determined

$$z = \frac{\{(h-\alpha x) + \alpha x\gamma_1\}(h-\alpha x)}{2(h-\alpha x) + \alpha x\gamma_1} \tag{3}$$

To get simple expression, h_α is introduced which is the length of elastic tensile region, that is

$$h_\alpha = h - z - \alpha x = \frac{(h-\alpha x)^2}{2(h-\alpha x) + \alpha x\gamma_1} \tag{4}$$

When all the moments produced by each stress block were summed, the resulted value is the resistant moment M_1 expressed as

$$M_1 = \frac{1}{6}\beta f_t\{2h_\alpha^{\,2} + h_\alpha(2z + 3\alpha x\gamma_1) + \alpha x\gamma_1(2z + m\alpha x)\} \tag{5}$$

Calculation of moment for specimen 2. The same procedure will bring us the final expression of resistant moment M_2, i.e.,

$$M_2 = \frac{1}{6}f_t\{2h_x^{\,2} + h_x(2y + 3x\gamma_2) + x\gamma_2(2y + mx)\} \tag{6}$$

Where y and h_x are

$$y = \frac{\{(h-x) + x\gamma_2\}(h-x)}{2(h-x) + x\gamma_2} \tag{7}$$

$$h_x = h - y - x = \frac{(h-x)^2}{2(h-x)+x\gamma_2} \tag{8}$$

Ratio of strength of specimen 1 to that of specimen 2. The experimental results tell that there is a strong relation between α, β and Wpx [10], that is,

$$\alpha x = W_{px} / (560\beta) \times 10^6 \tag{9}$$

When α and β are equal to 1.0, which is the case for specimen 2, x can be determined. Then the ratio of Wpx between specimen 1 and specimen 2 is

$$[W_{px}]_{Ratio} = \alpha\beta \tag{10}$$

At first, Wpx and β are obtained from experimental TSD. Then α can be got from Eq. 9. TSD is used to calculate γ_1 (specimen 1) and γ_2 (specimen 2) again. Then we can get y and z from Eq. 3 and Eq. 7, which leads us to getting h_x and h_α with employing Eq. 4 and Eq. 8. Finally M1 and M2 are calculated with Eq. 5 and Eq. 6.

The important point here is that M1 and M2 are determined by the information got only from TSD. The ratio of M1 to M2 is equal to the ratio of bending strength, because the ligament depths of both specimens are the same.

Table 4 shows the calculated ratio of M1/M2 for each type including the values necessary for the calculation, i.e., α, β and γ. Also the stress distribution models for typical specimen at the maximum load are depicted in Fig. 6, where we can observe the shape of stress block, the height of cracked region and the maximum compressive stress. The important observation here is that the height of neutral axis is about 0.6 for all of the specimens without large difference, though the height of cracked region, ft and fc are considerably different from each other.

Table 4 α, β, γ and M_1/M_2

	β	α	γ	M_1/M_2
N1	0.965	1.573	0.774	0.862
N2	1.000	1.000	1.002	1.000
N3	1.030	1.730	0.624	0.768
J1	0.820	1.122	0.812	0.742
J2	0.786	1.218	0.859	0.779
J3	0.673	2.083	0.761	0.616
E1	0.410	2.154	1.100	0.484
E2	0.554	1.454	1.024	0.642
E3	0.461	2.389	0.895	0.547
FS1	0.298	2.661	0.717	0.267
FS2	0.410	1.731	0.743	0.339
FS3	0.298	3.314	0.959	0.327
R1	0.915	0.449	1.088	0.919
R2	0.803	0.823	0.729	0.707
R3	0.781	1.197	0.735	0.675
SP1	0.516	0.711	0.797	0.517
SP2	0.494	0.911	0.784	0.487
SP3	0.429	1.752	0.565	0.337

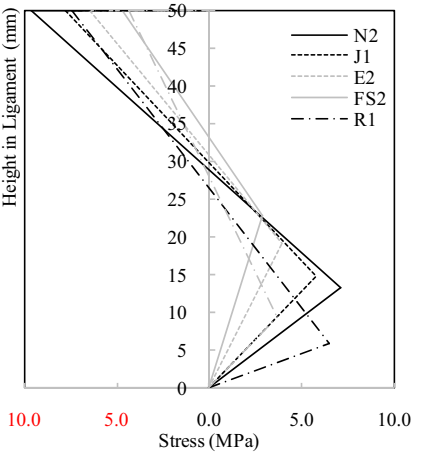

Fig. 6 Stress distribution models at maximum load

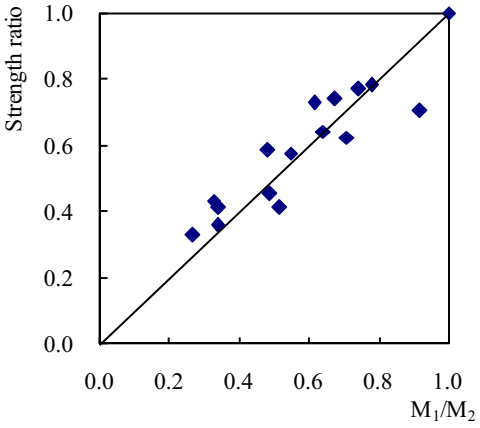

Fig. 7 Relationship between predicted and experimental bending moment

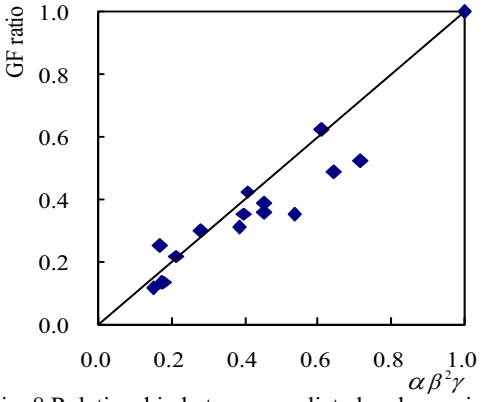

Fig. 8 Relationship between predicted and experimental fracture energy

Consistency of the Proposed Model

Comparison of bending moments. A comparison between experimental bending moments and ones predicted by the proposed model is depicted in Fig.7, which shows a good agreement between experimental and predicted ones indicating 0.91 as a correlation coefficient.

Comparison of fracture energy. Because GFpx is proportional to GF as we observed in Fig. 4, the ratio of GF of specimen 1 to that of specimen 2 can be predicted by the ratio of GFpx. Using Eq. 10, the ratio of GF can be expressed as

$$\left[GF_{px}\right]_{Ratio} = \left[W_{px}\right]_{Ratio} \times \beta \times \gamma = \alpha\beta^2\gamma \tag{11}$$

Fig. 8 shows the experimental GF and the predicted ones calculated by Eq. 11, which indicates good agreement indicating 0.94 as a correlation coefficient. The important finding is that GF is proportional to the second power of tensile strength (β ft) from Eq. 11. The results tell that the key to enhance GF is achieving high tensile strength of the placing joint.

Conclusions

The authors conducted fracture mechanics test of six types of concrete prisms which have a vertical placing joint. Tension softening diagrams were obtained, which were used to make a stress distribution model on the joint surface.

The authors proposed a stress distribution model which can predict both bending strength and fracture energy with using the information got only from TSD. The model was used to predict bending moment and fracture energy of six types of 18 specimens that have a placing joint in it. The predicted results showed a good agreement with the experimental ones.

References

[1] H. Mihashi: Survey of Fracture Mechanics of Concrete, Concrete Journal, 25(2), 14-25, (1987).

[2] K. Yamada, A. Satoh, S. Ishiyama: Evaluation of adhesion characteristics of joint in concrete by tension softening properties, Proceedings of "Fracture Mechanics of Concrete and Concrete Structure" , 3, 1753-1759, (2007).

[3] A. Satoh, K. Yamada and S. Ishiyama: A Discussion on Tension Softening Characteristics and Fracture Process of Concrete Prism with a Vertical Placing Joint, Proceedings of AIJ Tohoku Branch, 70, 49-54, (2007).

[4] K. Yamada and H. Mihashi: A Mechanism Leading to High Ductility for Extruded Cementitious Composite Reinforced with Polypropylene Short Fiber, Journal of Structure and Construction Engineering, AIJ, 520, 1-8, (1999).

[5] K. Yamada, H. Mihashi, N. Itagaki andS. Ishiyama: Stochastic Study on Size Effect in Tensile Strength of Short-Fiber Reinforced Cementitious Composite, Journal of Structure and Construction Engineering, AIJ, 540, 7-12, (2001).

[6] RILEM Draft Recommendation: Determination of the Fracture Energy of Mortar and Concrete by Means of Three-point bend Tests on Notched Beams, Materials and Structures, 18(106), 285-290, (1985).

[7] JCI: Izumi, I. (eds), Test method for fracture energy of plain concrete (Draft) in JCI standards, JCI, Tokyo, (2004).

[8] T. Kurihara, T. Ando, Y. Uchida and K. Rokugo: Evaluation of adhesive performance of construction joint in concrete by tension softening diagram, Proceedings of annual meeting of JCI, 18(2) 461-466, (1996).

[9] K. Yamada and H. Mihashi: A Proposition of Prediction Methods on Bending Behavior of Short-Fiber Reinforced Cementitious Composite, Proceedings of Symposium for Material Design and Performance of Concrete Structure, 339-346, (1999).

[10] A. Satoh, K. Yamada and S. Ishiyama: A Proposition of Stress Distribution Model in Section of Concrete Prism with a Vertical Placing Joint, Proceedings of annual meeting of JCI, in print, (2008).